

Understanding the total width of the 3_1^- state in $^{12}\text{C}^*$

K. C. W. Li,^{1,†} R. Neveling,² P. Adsley,^{3,4} H. Fujita,⁵ P. Papka,^{2,6} F. D. Smit,²
J. W. Brümmer,^{2,6} L. M. Donaldson,^{2,7} M. N. Harakeh,⁸ Tz. Kokalova,⁹
E. Nikolskii,¹⁰ W. Paulsen,¹ L. Pellegrini,^{2,7} S. Siem,¹ and M. Wiedeking^{2,7}

¹*Department of Physics, University of Oslo, N-0316 Oslo, Norway*

²*Themba LABS, National Research Foundation, PO Box 722, Somerset West 7129, South Africa*

³*Department of Physics and Astronomy, Texas A&M University, College Station, Texas 77843, USA*

⁴*Cyclotron Institute, Texas A&M University, College Station, Texas 77843, USA*

⁵*Research Center for Nuclear Physics, Osaka University, Ibaraki, Osaka 567-0047, Japan*

⁶*Department of Physics, University of Stellenbosch, Private Bag X1, 7602 Matieland, South Africa*

⁷*School of Physics, University of the Witwatersrand, Johannesburg 2050, South Africa*

⁸*Nuclear Energy Group, ESRIG, University of Groningen, 9747 AA Groningen, The Netherlands*

⁹*School of Physics and Astronomy, University of Birmingham,*

Edgbaston, Birmingham, B15 2TT, United Kingdom

¹⁰*NRC Kurchatov Institute, Ru-123182 Moscow, Russia*

(Dated: January 31, 2024)

Background: Recent measurements indicate that the previously established upper limit for the γ -decay branch of the 3_1^- resonance in ^{12}C at $E_x = 9.641(5)$ MeV may be incorrect. As a result, the 3_1^- resonance has been suggested as a significant resonance for mediating the triple- α reaction at high temperatures above 2 GK. Accurate estimations of the 3_1^- contribution to the triple- α reaction rate require accurate knowledge of not only the radiative width, but also the total width.

Purpose: In anticipation of future measurements to more accurately determine the γ -decay branch of the 3_1^- resonance, the objective of this work is to accurately determine the total width of the 3_1^- resonance.

Method: An evaluation was performed on all previous results considered in the current ENSDF average of 46(3) keV for the physical total width (FWHM) of the 3_1^- resonance in ^{12}C . A new **R**-matrix analysis for the 3_1^- resonance was performed with a self-consistent, simultaneous fit of several high-resolution ^{12}C excitation-energy spectra populated with direct reactions.

Results: The global analysis performed in this work yields a formal total width of $\Gamma(E_r) = 46(2)$ keV and an observed total width of $\Gamma_{\text{obs}}(E_r) = 38(2)$ keV for the 3_1^- resonance.

Conclusions: Significant unaccounted-for uncertainties and a misstated result were discovered in the previous results employed in the ENSDF for the physical (or observed) total width of the 3_1^- resonance. These previously reported widths are fundamentally different quantities, leading to an invalid ENSDF average. An observed total width of $\Gamma_{\text{obs}}(E_r) = 38(2)$ keV is recommended for the 3_1^- resonance in ^{12}C . This observed total width should be employed for future evaluations of the observed total radiative width for the 3_1^- resonance and its contribution to the high-temperature triple- α reaction rate.

I. INTRODUCTION

At high temperatures of above 2 GK, the triple- α reaction proceeds through resonances above the Hoyle state. Such high-temperature conditions are significant for astrophysical environments such as the shock front of type II supernovae. In this temperature region, there is significant uncertainty in the triple- α rate, owing to the complexities of disentangling the broad resonances which intrinsically overlap and interfere [1–7]. In contrast, the triple- α reaction at medium temperatures (between 0.1 and 2 GK) proceeds almost exclusively through the narrow primary peak of the Hoyle state. In order to understand the significance of correctly including the broader

resonances above the Hoyle state for the triple- α rate at high temperatures, consider the differences in the triple- α rates calculated by Angulo *et al.* and Fynbo *et al.* [8, 9]. At the time of publication of both Refs. [8] and [9], the 2_2^+ resonance was not yet conclusively observed. Consequently, the 2_2^+ resonance was omitted in the revised rate [9]. In contrast, the NACRE rate [8] assumed the existence of the 2_2^+ resonance at $E_x = 9.1$ MeV with $\Gamma = 0.56$ MeV, yielding an increase in the triple- α rate (above ≈ 6 GK) by several orders of magnitude relative to Ref. [9]. In the past few decades, the nuclear-physics community has invested significant effort in the search for the 2_2^+ rotational state, culminating in its eventual identification [3, 10–13]. Whilst this state has now been firmly established to exist at $E_x \approx 9.9$ MeV, its exact properties are still somewhat uncertain due to it being submerged under the broad, surrounding 0^+ strength.

An even greater source of uncertainty exists in the triple- α rate at high temperatures above 2 GK, where the

* Formerly: The chronicles of the 3_1^- total width in ^{12}C : the formal, the observed and the FWHM

† k.c.w.li@fys.uio.no

Gamow window enables the reaction to proceed through the 3_1^- resonance in ^{12}C . In the past, the contribution from the 3_1^- resonance has been largely neglected given the reported upper limit on the radiative branching ratio of $\Gamma_{\text{rad}}/\Gamma < 8.3 \times 10^{-7}$ (95% C.L.) [14]. Recent measurements have indicated that this upper limit may be incorrect. The first indication of this possible error was reported in a study by Tsumura *et al.* [15] which yielded a branching ratio of $\Gamma_{\text{rad}}/\Gamma = 1.3_{-1.1}^{+1.2} \times 10^{-6}$, though the resolution in Ref. [15] for the 3_1^- resonance was low (≈ 800 keV FWHM) and the identification/quantification of the 3_1^- peak is difficult given the complex and significant background. Specifically, it is the branching ratio for the $E1$ γ -ray transition between the 3_1^- and 2_1^+ states which is expected to dominate the total γ decay of the 3_1^- resonance; the probability of the $E3$ γ decay ($3_1^- \rightarrow 0_{\text{g.s.}}^+$) being determined in Ref. [15] as $6.7(10) \times 10^{-9}$ using the associated $0.31(4)$ meV width from an (e, e') measurement [16] and the ENSDF average for the total width of the 3_1^- resonance of $\Gamma = 46(3)$ keV [17]. Since 2017, the ENSDF average for the 3_1^- total width has employed Refs. [18–21], yielding an uncertainty-weighted average of $46(3)$ keV [17] (see Table I). A subsequent result of $\Gamma_{\text{rad}}/\Gamma = 6.4(51) \times 10^{-5}$ was reported by Cardella *et al.* [25], however, the resolution is also relatively low and only ≈ 3 counts corresponding to the 3_1^- resonance were observed. Unfortunately, the uncertainties from both measurements are substantial and lead to large uncertainties in the associated contribution to the triple- α rate at high temperatures. However, what is clear is that if the order of magnitude of these results is correct, the previously established upper limit of $\Gamma_{\text{rad}}/\Gamma < 8.3 \times 10^{-7}$

TABLE I. The reported results for the 3_1^- resonance in ^{12}C which are employed in the current ENSDF average [17]. The ENSDF definition for the listed total width is the full width at half maximum (FWHM) intensity for a resonance. $\Gamma(E_r)$ is the formal total width (see Eq. 3). Γ_{obs} is the observed total width (see Eq. 8). Γ_{FWHM} is the FWHM of the intrinsic lineshape. Averaging the total widths reported in Refs. [18–21] yields an average of $45(3)$ keV; this minor discrepancy with the currently listed $46(3)$ keV is “due to a rounding judgment” [22]. Details of the uncertainty policy for the ENSDF can be found in Refs. [23, 24]).

Ref.	Resolution ^a [keV]	$\Gamma(E_r)$ [keV]	$\Gamma_{\text{obs}}(E_r)$ [keV]	Γ_{FWHM} [keV]
Douglas <i>et al.</i> [18]	—	—	—	30(8)
Browne <i>et al.</i> [19]	≈ 40	—	—	36(6) ^b
Alcorta <i>et al.</i> [20]	60–120 55–85	—	—	43(4)
Kokalova <i>et al.</i> [21]	54(2) ^c	48(2)	—	—

^a Reported as FWHM.

^b The abstract and body of Ref. [19] inconsistently report 35(6) and 36(6) keV, respectively; the ENSDF employs the latter [17].

^c Determined from Ref. [21] which incorrectly reports the Gaussian standard deviation of $\sigma = 23(1)$ keV as the FWHM.

(95% C.L.) may be incorrect. The upward trend for the associated radiative branching ratio for the 3_1^- resonance [15, 25] suggests that the 3_1^- contribution may not only be significant, but dominant at temperatures above 2 GK. The significant uncertainties in Refs. [15, 25] do not enable the 3_1^- contribution to be meaningfully constrained and new, more sensitive measurements are required. Accurate estimations for the observed total radiative width of the 3_1^- resonance, as well as its contribution to the triple- α reaction rate, require accurate knowledge of not only the γ -decay branching ratio, but also the total width. In anticipation of future measurements to more accurately determine the γ -decay branch, the primary objective of this work is to provide a new analysis for the total width of the 3_1^- resonance. A secondary objective is to perform a meta-analysis on the previous results considered in the current ENSDF average for the 3_1^- total width.

II. DATA ANALYSIS AND RESULTS

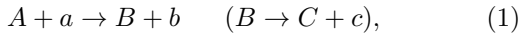
In this work, the primary analysis considers inclusive excitation-energy spectra from six different measurements (see Table II). The $^{12}\text{C}(\alpha, \alpha')^{12}\text{C}$ and $^{14}\text{C}(p, t)^{12}\text{C}$ data have been previously employed in a previous investigation for the predicted breathing-mode excitation of the Hoyle state [6, 7]. The $^{12}\text{C}(p, p')^{12}\text{C}$ spectrum studied in this work is an independently analysed subset of the data employed in a previous study of the 3_1^- total width [21]. These spectra were simultaneously fitted with phenomenological lineshape parameterizations from multi-level, multi-channel \mathbf{R} -matrix theory. The underlying formalism of the fit analysis is detailed in Section II A and the details of this primary analysis are presented in Section II B. In addition, a meta-analysis was also performed on the previous studies considered on this current ENSDF average [17], with the exception of Ref. [18]. These assessments are detailed in sections II C, II D and II E. A quantitative assessment of the 3_1^- total width reported in Ref. [18] was deemed unfeasible within the scope of this work as the methodology in Ref. [18] is significantly different from this work.

TABLE II. Summary of the experimental parameters for the inclusive excitation-energy spectra analysed in this work.

Reaction	Angle [deg]	E_{beam} [MeV]	Target ($\mu\text{g}/\text{cm}^2$)	Fitted E_x range [MeV]
$^{12}\text{C}(\alpha, \alpha')^{12}\text{C}$	0	118	^{12}C (1053)	5.0–14.8
	0	160	^{12}C (300)	7.3–20.0
	10	196	^{12}C (290)	7.15–21.5
$^{14}\text{C}(p, t)^{12}\text{C}$	0	100	^{14}C (280)	6.0–15.3
	21	67.5	^{14}C (300)	6.8–14.5
$^{12}\text{C}(p, p')^{12}\text{C}$	16	66	^{12}C (1000)	6.0–15.3

A. R-matrix formalism

A comprehensive description of the phenomenological **R**-matrix formalism for this analysis is given in Ref. [7], with the pertinent components described here. For this analysis of direct-reaction data, consider a direct reaction populating a recoil nucleus which subsequently decays, represented as



for the target (A), projectile (a), recoil (B), ejectile (b) and decay products from the recoil (C and c). The intrinsic lineshape observed for excitations of a particular spin and parity is given by

$$N_{ab,c}(E) = P_c \left| \sum_{\lambda,\mu}^N G_{\lambda ab}^{\frac{1}{2}} \gamma_{\mu c} A_{\lambda\mu} \right|^2, \quad (2)$$

where γ is the reduced-width amplitude and $A_{\lambda\mu}$ is an element of the level matrix. Subscript ab denotes the $A + a \rightarrow B + b$ reaction channel and subscript c denotes the $B \rightarrow C + c$ decay channel. P_c is the penetrability of the decay channel and the feeding factor, G_{ab} , captures the population strength and excitation-energy dependence for the incoming reaction channel (see Ref. [7] for details). The total width of the μ^{th} level is expressed as a sum over the decay-channel widths

$$\Gamma_{\mu}(E) = \sum_{c'} 2\gamma_{\mu c'}^2 P_{c'}(\ell, E), \quad (3)$$

where γ^2 is the reduced width and c' is a summation index over the decay channels. The penetrability for decay channel c , with an orbital angular momentum of the decay, ℓ , is expressed as

$$P_c(\ell, E) = \frac{ka_c}{F_l(\eta, ka_c)^2 + G_l(\eta, ka_c)^2}, \quad (4)$$

where $F_l(\eta, ka_c)$ and $G_l(\eta, ka_c)$ are the regular and irregular Coulomb functions, respectively; k is the wavenumber, a_c is the fixed channel radius and η is the dimensionless Sommerfeld parameter [26].

In the case of an isolated resonance, the corresponding lineshape corresponds to a single-level approximation [27] of the form

$$N_{ab,c}(E) = \frac{G_{ab}\Gamma_c}{(E - E_r - \Delta)^2 + \frac{1}{4}\Gamma^2}, \quad (5)$$

where E_r is the resonance energy and $\Delta \equiv \Delta_{11}$ is expressed as a sum over the decay channels, and

$$\Delta_{\lambda\mu} = \sum_{c'} -(S_{c'} - B_{c'})\gamma_{\lambda c'}\gamma_{\mu c'}, \quad (6)$$

where S_c and B_c are the shift factors and boundary condition parameters, respectively. For this work, the ‘‘natural’’ boundary condition, $B_c = S_c(E_r)$, was employed. The shift factors are expressed as

$$S_l(E) = \frac{ka_c [F_l(\eta, ka_c)F_l'(\eta, ka_c) + G_l(\eta, ka_c)G_l'(\eta, ka_c)]}{F_l(\eta, ka_c)^2 + G_l(\eta, ka_c)^2}, \quad (7)$$

where F_l' and G_l' are the derivatives of the regular and irregular Coulomb functions, respectively.

As this study is focused on precisely extracting the physical total width of the 3_1^- resonance, it is important to understand the nuances between the various width definitions relevant to **R**-matrix analyses. For the case of an isolated resonance, the full width half maximum (FWHM) for the intrinsic lineshape of a resonance is referred to as the physical (or intrinsic) total width. The physical total width is model independent and corresponds to the ENSDF definition of the total width. The formal total width (Eq. 3) is a highly model-dependent **R**-matrix quantity which is correlated with, yet distinct from the physical total width. This is predominantly due to the energy dependence of the energy shift (Δ) in Eq. 5. However, for a given formal total width, the corresponding physical total width can be well approximated by what is known as the observed total width, defined as

$$\Gamma_{\text{obs},\mu}(E) = \frac{\sum_{c'} 2\gamma_{\mu c'}^2 P_{c'}(\ell, E)}{1 + \sum_{c'} \gamma_{\mu c'}^2 \frac{dS_{c'}}{dE} \Big|_{E=E_r}}. \quad (8)$$

This approximation is valid under the aforementioned natural boundary condition, and the approximation of the shift factor to be linear in the vicinity of the resonance energy (known as the Thomas approximation [27]) as:

$$\Delta_{\mu}(E) \approx \Delta_{\mu}(E_r) + (E_r - E) \sum_{c'} \gamma_{\mu c'}^2 \frac{dS_{c'}}{dE} \Big|_{E=E_r}. \quad (9)$$

As long as the shift factor and penetrability vary slowly over the resonance range, the observed total width well approximates the physical total width for a Breit-Wigner resonance. The formal total width is therefore a fundamentally different quantity from the observed total width and the physical total width (FWHM) of an isolated resonance; the latter two widths converging when the Thomas approximation is accurate. This Thomas approximation is poor for highly clustered resonances located near particle threshold (an example is given in Section II C 1). In such cases, the corresponding shift factors are significantly non-linear across the range of the resonance and the reduced widths are large, which further amplifies the effect of the $\Delta_{\lambda\mu}$ parameter (see Eq. 6). In general, the formal total width should therefore not be compared with the physical width observed for a resonance (although these quantities can be very similar under certain conditions). This feature for this parameterization of **R**-matrix theory has been detailed in the seminal work of Lane and Thomas [27] as well as in more recent studies such as Refs. [28, 29]. It is therefore standard practice for only the physical resonance properties (i.e. the observed parameters) to be stored in evaluated

nuclear data libraries such as the ENSDF. This ensures the portability of results between different analyses (e.g. for ENSDF evaluations), which often employ different channel radii to produce formal parameters which cannot be directly compared. This is particularly appropriate for \mathbf{R} -matrix parameterizations, for which there is no particular “correct” channel radius, rather a range of channel radii (related to the physical particles sizes of the partition) which enable data to be well parameterized. In the context of \mathbf{R} -matrix cross-section calculations for nuclear astrophysics, it is standard to treat the ENSDF parameters as observed parameters. These evaluated quantities can then be transformed to their formal counterparts for any particular channel radius for subsequent calculations. For completeness, the \mathbf{R} -matrix formalism discussed thus far, that requires the choice of arbitrary boundary condition and channel-radius parameters, corresponds to the Wigner-Eisenbud parameterization of \mathbf{R} -matrix theory. Alternative \mathbf{R} -matrix parameterisations have been proposed by Brune [30], as well as Ducru and Sobes [31], which elegantly mitigate ambiguities stemming from these arbitrary parameters. However, the Wigner-Eisenbud parameterization applied in this work is still widely employed.

B. The primary analysis of inclusive spectra

In this work, a simultaneous, self-consistent analysis was performed on the data corresponding to Table II. The two main contributions to the broad underlying background are the 2_2^+ rotational excitation of the Hoyle state as well as an intricate monopole strength which consists of the ghost of the 0_2^+ Hoyle state as well as the 0_3^+ and 0_4^+ resonances (see Ref. [6, 7] for a recent experimental investigation). The 0_3^+ resonance at $E_x \approx 9$ MeV has been suggested to correspond to the breathing-mode excitation of the Hoyle state [32–37], with the higher-energy 0_4^+ excitation mode at $E_x \approx 11$ MeV corresponding to a predicted bent-arm 3α structure [5, 35, 38–40]. Two versions of the fits were also explored: the first implements the standard prescriptions for the penetrability and shift factor (Eqs. 4 and 7) which assume the ^8Be daughter states to be infinitesimally narrow. The second accounts for the intrinsic widths of the ^8Be states (see Ref. [7] for details). To investigate the channel-radius dependence for the 3_1^- resonance, a range of channel radii from $a_c = 4$ to 11 fm was explored in 0.1 fm increments. In these fits, the Wigner limit was applied to the α_1 decay channel of the 3_1^- resonance as the corresponding branching ratio is known to be extremely small [20, 41, 42]. The optimal fit results from the simultaneous analysis of all the data corresponding to Table II are presented in Fig. 1 and Table III, yielding $\Gamma(E_r) = 46(2)$ keV with $\Gamma_{\text{obs}}(E_r) = 38(2)$ keV for the 3_1^- resonance.

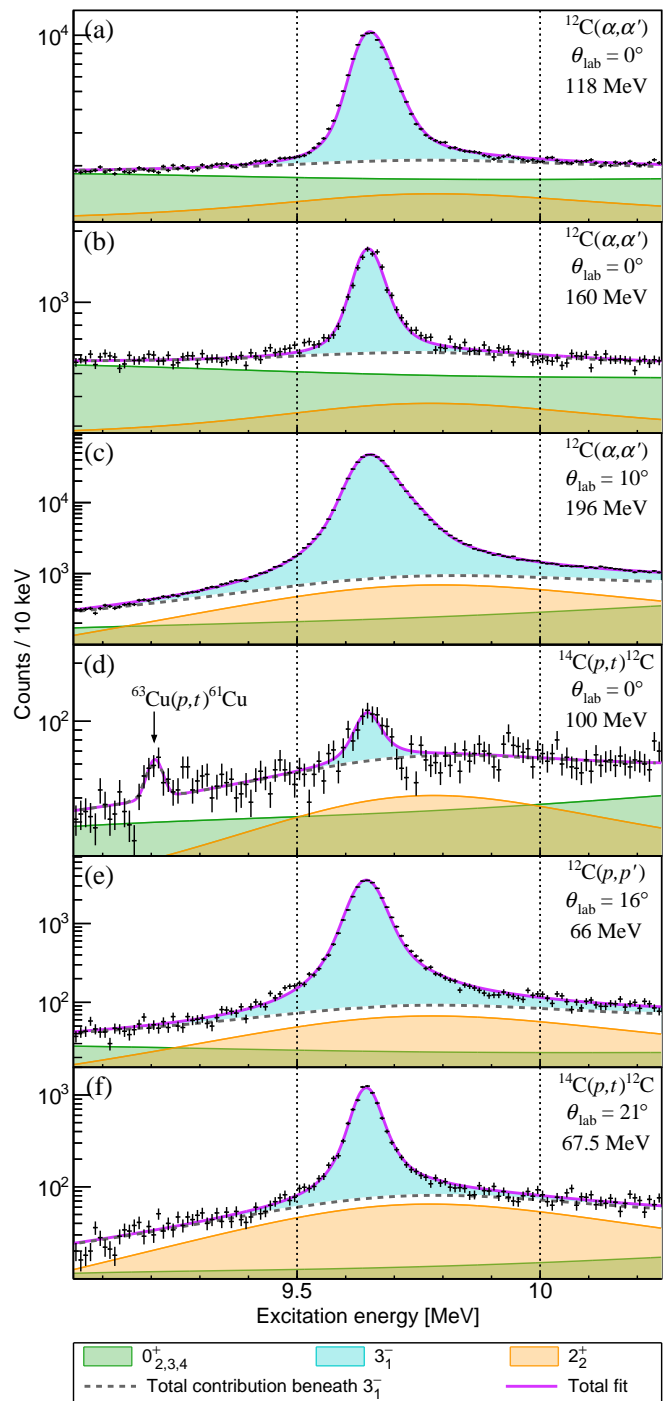


FIG. 1. (Color online) Decomposition of the optimal fit for the inclusive excitation-energy spectra. On each spectrum, the 3_1^- resonance is superimposed on the total contribution from all other resonances and the instrumental background. For each spectrum, the reaction, measurement angle and beam energy are indicated in the top right of the corresponding panel. On panel (d), the contaminant state from ^{63}Cu ($E_x = 4.756$ MeV) is indicated; see Ref. [7] for details of the contaminants.

TABLE III. Optimized fit results for the global analysis of all considered data (see Fig. 1).

${}^8\text{Be}^a$	AIC ^b	E_r [MeV]	α_0 decay			α_1 decay			Total width		
			a_{α_0} [fm]	$\theta_{\alpha_0}^2$	$\Gamma_{\alpha_0}(E_r)$ [keV]	a_{α_1} [fm]	$\theta_{\alpha_1}^2$ ^c	$\Gamma_{\alpha_1}(E_r)$ [keV]	$\Gamma(E_r)$ [keV]	$\Gamma_{\text{obs}}(E_r)$ [keV]	Γ_{FWHM} [keV]
Discrete	15088	9.641(2)	4.8	0.291(2)	46(2)	4.8	0.0(1)	0(2)	46(2)	38(2) ^d	38(2)
Finite	15179	9.641(2)	4.8	0.316(3)	47(2)	4.8	0.00(7)	0(2)	47(2)	39(2)	39(2)

^a This indicates the prescription employed for the penetrability and shift factor: “Discrete” is the standard prescription which assumes the ${}^8\text{Be}$ states to be infinitely narrow. “Finite” indicates that the intrinsic widths of the ${}^8\text{Be}$ states were accounted for [7].

^b The AIC estimator is used to determine the best quality model as maximum likelihood estimation is employed to fit the data.

Minimum chi-square estimation is not used as there are several regions in the spectra which have very low counts (< 10); Ref. [7]

presents the full fit ranges for a subset of the considered data.

^c The Wigner limit is applied for the α_1 decay channel; see text for details.

^d Corresponds to the optimal fit for the 3_1^- resonance in this work.

C. Assessing the 3_1^- total width from Ref. [21]

To assess the 3_1^- total width reported by in Ref. [21], an isolated analysis was performed on the subset of the ${}^{12}\text{C}(p, p'){}^{12}\text{C}$ data from Ref. [21]. These ${}^{12}\text{C}(p, p'){}^{12}\text{C}$ data are the same that were included in the primary analysis of this work (see Section II B and Table II). This analysis was repeated for a ${}^{14}\text{C}(p, t){}^{12}\text{C}$ excitation-energy spectrum with better resolution to confirm whether the same observed systematic trends are independent of the data (see Section II C 2).

1. Isolated analysis of ${}^{12}\text{C}(p, p'){}^{12}\text{C}$ data

Ref. [21] reported only the formal total width for the 3_1^- resonance, which was incorrectly compared to the physical total width of the state reported in other works currently employed in the ENSDF average [18–20]. As previously mentioned in Section II A, the formal total width is a model-dependent quantity which is distinct from the physical total width (FWHM) of a resonance. Consequently, this misstated formal total width of $\Gamma = 48(2)$ keV reported by Ref. [21] was mistakenly considered in the ENSDF average for the physical total width (FWHM) of the 3_1^- resonance [17]. The current ENSDF average is thus invalid for determining the observed total radiative width for the 3_1^- resonance. Determining the observed total radiative width requires knowledge on the observed total width, in addition to the $E1$ ($3_1^- \rightarrow 2_1^+$) γ -decay branching ratio and the physical $E3$ ($3_1^- \rightarrow 0_{\text{g.s.}}^+$) γ -decay width of $0.31(4)$ meV [16] (see Ref. [15] for a more detailed discussion). To clarify why this misstated result is particularly problematic for the 3_1^- state in ${}^{12}\text{C}$, an analysis is given: panels (a) and (b) of Fig. 2, present the channel-radius dependence of the 3_1^- intrinsic lineshapes with the formal and observed total widths being kept constant at 40 keV, respectively. The clear channel-radius dependence of the formal width is apparent, in contrast to the observed total width which is weakly dependent of the channel radius. This effect

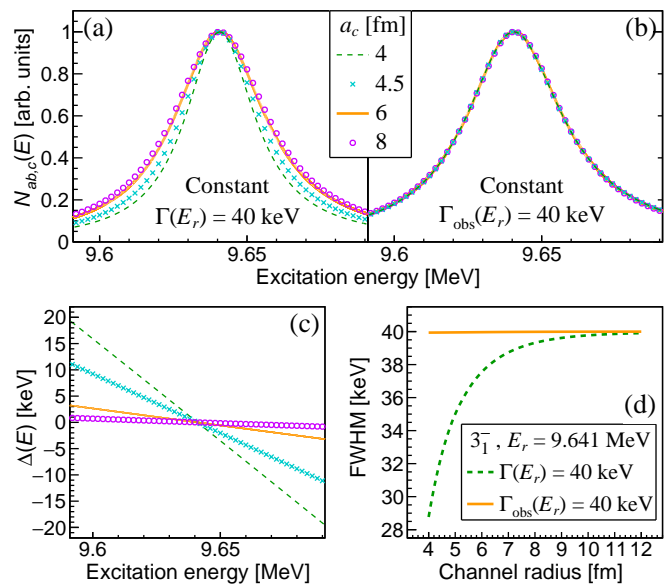


FIG. 2. (Color online) The channel-radius dependence of the 3_1^- resonance for the intrinsic lineshape with (a) constant $\Gamma(E_r) = 40$ keV, (b) constant $\Gamma_{\text{obs}}(E_r) = 40$ keV, (c) the energy shift and (d) the FWHM of the intrinsic lineshape.

is predominantly due the channel-radius dependence of the shift function near the α_0 decay threshold. In general, the shift function at a particular energy becomes more constant towards larger channel radii (equivalently for the energy shift, Δ) and thus, the formal total width converges with the observed total width at large channel radii, as shown in panels (c) and (d) of Fig. 2.

For completeness, a counter example for the channel-radius independence of the observed total width (defined in Eq. 8) is provided by the broad 2_2^+ rotational excitation of Hoyle state which underlies the 3_1^- resonance, see Fig. 3. Over the broad range of the 2_2^+ resonance, which has an experimentally observed FWHM of ≈ 1 MeV, the energy shift is observed to be non-linear. Over the range of explored channel radii shown in Fig. 3, the Thomas approximation is inappropriate for the 2_2^+

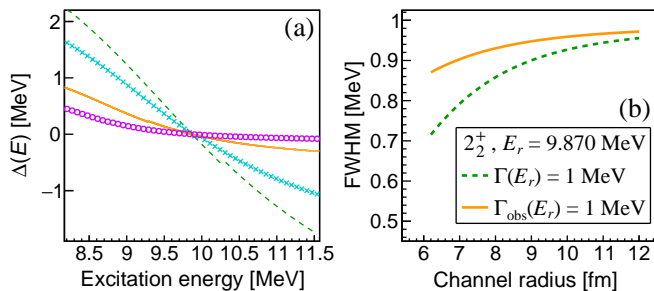


FIG. 3. (Color online) The channel-radius dependence of the 2_2^+ resonance for (a) the energy shift and (b) the numerically determined FWHM of the intrinsic lineshape.

resonance and thus, $\Gamma_{\text{obs}}(E_r)$ is no longer an accurate measure for the intrinsic FWHM of the resonance. This general effect manifests strongly for resonances which are located near a particle threshold and exhibit significant clustering (i.e., large reduced widths). For such cases, we thus encourage the reporting of not only the formal and observed width, but also the FWHM (Γ_{FWHM}) to facilitate model independence in comparisons to data and between analyses. For \mathbf{R} -matrix derived lineshapes, the FWHMs reported in this work are numerically determined for the intrinsic lineshape. For Γ_{FWHM} to be consistent between different direct-reaction datasets, Γ_{FWHM} is determined for intrinsic lineshapes without feeding factors.

In this work, the formal total width of the 3_1^- resonance of $\Gamma(E_r) = 48(2)$ keV reported by Ref. [21] has been converted to the observed total width of $\Gamma_{\text{obs}}(E_r) = 39(4)$ keV which is appropriate for the ENSDF average. This observed total width matches the numerically determined FWHM of $\Gamma_{\text{FWHM}} = 39(4)$ keV (see Table I). The overall uncertainties for these converted values include previously unaccounted-for systematic errors stemming from the approximations employed in Ref. [21]. To estimate these unaccounted-for systematic errors, a comprehensive, isolated analysis was also performed on the subset of the data employed in Ref. [21]. This subset exhibits a better experimental resolution of $48(1)$ keV (FWHM) and fewer experimental artefacts than in Ref. [21]. The study of Ref. [21] parameterized the intrinsic lineshape for the 3_1^- resonance with that of a single, isolated level (Eq. 5). This is a reasonable approximation given the relatively narrow width of ≈ 40 keV with respect to the next closest 3^- resonance at $E_x = 18350(50)$ keV. Furthermore, the single (decay) channel approximation employed by Ref. [21] is appropriate as the 3_1^- resonance is understood to decay almost exclusively through the α_0 ($\ell = 3/f$ -wave) decay channel to the 0^+ ground state of ^8Be [20, 41, 42]. The \mathbf{R} -matrix-derived lineshape employed in Ref. [21] is functionally the same as Eq. 5, with Ref. [21] having employed a degenerate sign difference in the definition of both Δ and the first term of the denominator in Eq. 5. Perhaps the most critical approximation made by Ref. [21] concerns the description

of the broad, background components beneath the 3_1^- resonance with a second-order polynomial and a 2^+ resonance situated at $E_x \approx 9.6$ MeV with $\Gamma \approx 600$ keV. The effect of target-related energy loss for the ejectile is also ignored. Finally, the feeding factor for the direct populating channel (G_{ab}) was also implicitly approximated to be constant. Ref. [21] also investigated whether the intrinsic 3_1^- lineshape can be well parameterized with a standard (symmetric) Lorentzian in comparison to the \mathbf{R} -matrix lineshape given by Eq. 5. In this investigation, we also consider the somewhat-common approximation of employing a pseudo \mathbf{R} -matrix lineshape where the energy shift (Δ in Eq. 5) is neglected. A systematic sensitivity study of these approximations was performed for both the intrinsic and experimentally observed lineshapes of the 3_1^- resonance, see Fig. 4. A Gaussian experimental resolution of $\sigma = 20$ keV was employed, which is similar to the $\sigma = 23(1)$ keV resolution reported in Ref. [21]. For the \mathbf{R} -matrix lineshape of Eq. 5, an observed

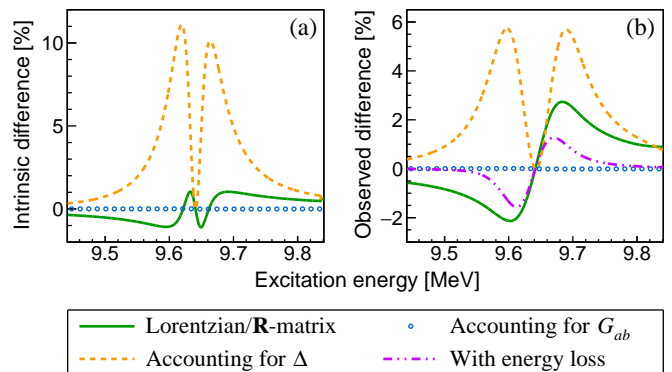


FIG. 4. (Color online) The differences in the (a) intrinsic and (b) experimentally observed lineshapes caused by the considered approximations (relative to the peak maximum). The observed lineshapes were produced by convoluting the intrinsic lineshapes with the experimental response observed in the $^{12}\text{C}(p, p')^{12}\text{C}$ data analyzed in this work.

total width of $\Gamma_{\text{obs}}(E_r) = 40$ keV at $E_r = 9.641$ MeV was employed. For the test of a standard (symmetric) Lorentzian, an energy-independent width of $\Gamma = 40$ keV was implemented. It is observed that the inclusion (or lack) of an energy-dependent feeding factor is negligible. This is unsurprising given the typical slowly-varying energy dependence of the feeding factor [7], which is well approximated to be constant over the ≈ 40 keV width of the 3_1^- resonance. The effects of employing a standard Lorentzian and neglecting the target-related energy loss are more significant given the small statistical errors for the high yields at the peak of the 3_1^- resonance in Ref. [21] (≈ 20000 counts per 5 keV bin). The $\Delta = 0$ approximation was observed to have the most dramatic effect on both the intrinsic and experimentally observed lineshape for the 3_1^- resonance. In general, this approximation is particularly poor for resonances near threshold which exhibit a high degree of clustering, and thus large

TABLE IV. Summary of analysis configurations and results for the $^{12}\text{C}(p,p')^{12}\text{C}$ reaction at $E_{\text{beam}} = 66$ MeV. χ_{red}^2 is the reduced chi-squared statistic. The Landau energy-loss parameters were fitted to the intrinsically narrow Hoyle state in the subset of $^{12}\text{C}(p,p')^{12}\text{C}$ data from Ref. [21] analyzed in this work. The channel radius for all **R**-matrix derived lineshapes is the same as that employed by Ref. [21]: $a_c = 1.3(4^{1/3} + 8^{1/3}) \approx 4.7$ fm. The reported errors contain the fitting errors and a minimum focal-plane detection error of 1 keV, added in quadrature, with no other systematic errors included (e.g., channel-radius dependence).

Case	Background	Intrinsic lineshape, 3_1^-	Energy shift, Δ	Energy loss	Feeding factors	χ_{red}^2	3_1^-			
							E_r [MeV]	$\Gamma(E_r)$ [keV]	$\Gamma_{\text{obs}}(E_r)$ [keV]	Γ_{FWHM} [keV]
(1)	Quadratic	R -matrix	✓			1.669	9.645(1)	54(1)	43(1)	43(1)
(2)	Quadratic + Gaussian	Lorentzian				7.209	9.646(1)	36(1)		36(1)
(3)	Quadratic + Gaussian	R -matrix				1.310	9.645(1)	41(1)	41(1)	41(1)
(4)	Quadratic + Gaussian	R -matrix	✓			1.341	9.645(1)	51(1)	41(2)	41(1)
(5)	Quadratic + Gaussian	R -matrix	✓	✓		1.321	9.644(1)	50(1)	41(2)	41(1)
(6)	Quadratic + Gaussian	R -matrix	✓	✓	✓	1.321	9.644(1)	50(1)	41(2)	41(1)
(7)	Quadratic + Lorentzian	R -matrix	✓			1.358	9.645(1)	51(1)	41(2)	41(1)
(8)	Quadratic + 2_2^+ (Eq. 5)	R -matrix	✓			1.269	9.645(1)	47(2)	38(2)	38(2)

reduced widths and quickly varying energy shifts. To clarify this, the $\Delta = 0$, pseudo **R**-matrix approximation to the intrinsic lineshape was not explored in Ref. [21], however it is detailed here as a caution for future studies which may seek to apply it. It is clear that several of these approximations may individually have a significant effect on the observed lineshape. However, the combined effect from these approximations on the extracted observed total width for the 3_1^- resonance is dependent on the features of the data. To gauge the systematic errors associated with these various approximations, an exhaustive test for various combinations of these approximations was performed on a subset of the $^{12}\text{C}(p,p')^{12}\text{C}$ data in Ref. [21] and the most revealing combinations are presented as different cases in Table IV. The associated fits were performed with χ_{red}^2 minimization given the limited fit range (which approximately matches that in Ref. [21]) in which the data is approximately normally distributed.

In terms of background systematics, it is observed that the choice of parameterization for the underlying 2_2^+ contribution is significant. First-order and second-order polynomial backgrounds were found to yield almost identical fits, thus the results from the former are omitted from Table IV.

- **Case (1):** The observed total width for the 3_1^- resonance is larger when approximating the underlying 2_2^+ resonance with simplified Gaussian and standard Lorentzian lineshapes and larger still when not including a broad component for the 2_2^+ resonance at all.
- **Case (2):** In terms of the lineshape for the 3_1^- resonance itself, a standard (symmetric) Lorentzian

lineshape [case (2)] yields a poor fit and exhibits a significantly smaller Γ_{FWHM} than other scenarios.

- **Case (3):** A comparison of case (3) to case (4) cases shows that ignoring the energy shift naturally affects the extracted formal width, however, the FWHM of the 3_1^- resonance is consistent.
- **Case (4):** This case most closely matches the fit methodology employed in Ref. [21] and the corresponding fit in Fig. 5 yielded $\Gamma(E_r) = 51(1)$ keV and $\Gamma_{\text{obs}}(E_r) = 41(2)$ keV, with the formal total width being in reasonable agreement with the corresponding value reported in Ref. [21] (see Table I). In this work, the formal total reported in Ref. [21] was converted to the appropriate observed total width for the ENSDF. By comparing the fit of case (4) to the best fit of case (8), the unaccounted-for systematic error due to the background approximation in Ref. [21] can be roughly estimated at 3 keV for both $\Gamma_{\text{obs}}(E_r)$ and Γ_{FWHM} . This error has been included for the corrected values of $\Gamma_{\text{obs}}(E_r) = 39(4)$ keV and $\Gamma_{\text{FWHM}} = 39(4)$ keV which we recommend for future evaluations which consider the result of Ref. [21].
- **Case (5):** The inclusion of the target-related energy loss improves the quality of the fit, however the extracted formal and observed widths are not strongly affected given the energy resolution of the data.
- **Case (6):** The feeding factors have a negligible effect on the fits in general. This is to be expected given the typical slowly-varying energy dependence of the feeding factor [7], which is well approximated

to be constant over the ≈ 40 keV width of the 3_1^- resonance.

- **Case (7):** Approximating the underlying 2_1^+ resonance as a symmetric Lorentzian yields a poorer fit in comparison to the Gaussian approximation for the 2_1^+ resonance in case (4). This may be due to the fact that the intrinsic shape of the 2_1^+ is asymmetric, with the low-energy tail being strongly suppressed by the penetrability; a feature that the longer tails of a Lorentzian (in comparison to a Gaussian) are less suited to approximate.
- **Case (8):** This provides the best fit of the considered cases, employing the single-level, single-channel approximation of Eq. 5 for both the 3_1^- resonance and the underlying broad 2_2^+ resonance, yielding a formal total width of $\Gamma(E_r) = 47(2)$ keV, with an observed total width of $\Gamma_{\text{obs}}(E_r) = 38(2)$ keV. To further emphasize the inappropriate nature of comparing the channel-radius dependent formal total width to the observed total width (see Fig. 2), a fit with case (8) using a channel-radius of 4 fm was performed as opposed to the choice of 4.7 fm (see caption of Table IV) in Ref. [21], yielding a much larger formal total width of $\Gamma(E_r) = 65(4)$ keV, whilst the observed total width of $\Gamma_{\text{obs}}(E_r) = 40(2)$ keV is in good agreement with the optimal fit in this work which yielded $\Gamma_{\text{obs}}(E_r) = 38(2)$ keV.

To emphasize the significant channel-radius dependence of the formal total width for the 3_1^- resonance (in contrast to the observed total width), fits were performed with case (4) over a range of channel radii from $a_c = 4$ to 8 fm in 0.1 fm increments (see Fig. 6). The optimal channel radius for this isolated fit was determined as $a_c = 4.5$ fm, with all explored channel radii providing a similar quality fit. As previously mentioned, whilst the difference between formal and observed widths can sometimes be quite small, the difference can be significant under certain conditions. This is precisely the case

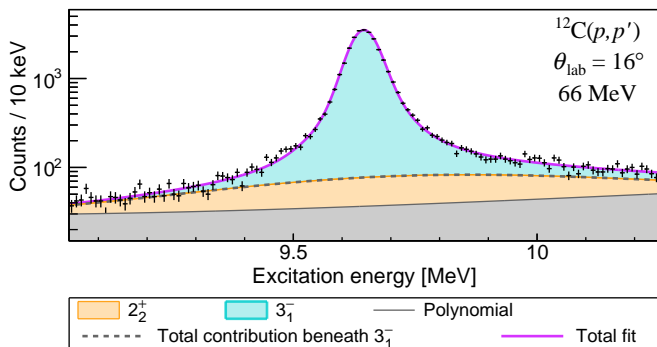


FIG. 5. (Color online) Decomposition of the fit for case (4) in Table IV. The 3_1^- resonance is superimposed on the total contribution of the 2_2^+ resonance (parameterized with a Gaussian lineshape) and a polynomial background. The reaction, measurement angle and beam energy are indicated.

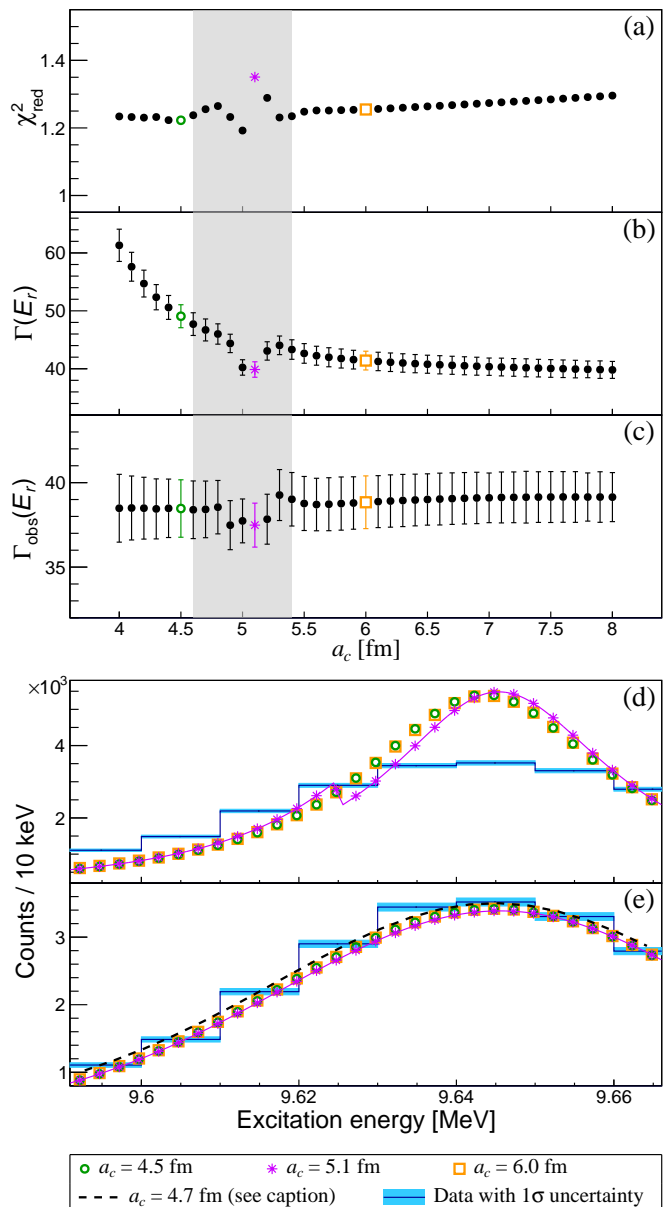


FIG. 6. (Color online) For the 3_1^- resonance: the channel-radius dependence of (a) χ^2_{red} , (b) $\Gamma(E_r)$ and (c) $\Gamma_{\text{obs}}(E_r)$. The range of channel radii which yield significant discontinuities (4.6–5.4 fm) is highlighted in filled gray. Panels (d) and (e) respectively present the intrinsic and observed lineshapes corresponding to the channel radii of 4.5, 5.1 and 6.0 fm (see legend), corresponding to panels (a)-(c). The fit results at different channel radii correspond to the fit conditions of case (4) (see Table 4), with the exception of $a_c = 4.7$ fm in panel (e) which includes the Landau energy loss of case (5).

for the 3_1^- resonance, for which a choice of $a_c = 4.0$ is demonstrated to describe the data similarly well in Fig. 6(a), would yield a formal width greater than 60 keV that is unrelated to the physical total width of the state. The observed fluctuations in the reduced chi-squared for some channel radii between $a_c = 4.6$ –5.4 fm is a consequence of

small numerical inaccuracies for the Coulomb functions calculated with the GNU Scientific Library (GSL) in this work [43]. As such, the fits with strongly-deviating channel radii (e.g. $a_c = 5.0$ – 5.2 fm) were disregarded as the numerical inaccuracies for these cases were more significant. An example of how these numerical inaccuracies affect the intrinsic and experimental lineshapes for the 3_1^- resonance is presented in Fig. 6(d) and (e), respectively. It is observed that the numerical error for $a_c = 5.1$ presents as a jagged “discontinuity” in the intrinsic lineshape near $E_x = 9.625$ MeV. The scale and location of these numerical inaccuracies are highly dependent on the affected a_c values, however, these features are generally more prevalent towards lower energies. For most cases, these numerical inaccuracies are orders of magnitude below the statistical errors of the considered data and therefore do not affect the conclusions of this work. This is supported by the intrinsic lineshapes for $a_c = 4.5$ and 6.0 fm which do not present such numerical discontinuities and are almost identical, see Fig. 6(d). Furthermore, it is observed that the observed lineshapes in Fig. 6(e), which include a Gaussian convolution, are in significantly better agreement than the 1σ uncertainty of the data. Nevertheless, the optimal fits presented in the primary analysis in Section II B were checked to not exhibit such numerical discontinuities in the range of the 3_1^- resonance. For future studies, an alternative algorithm detailed is planned to be implemented for lower-energy resonances where data may warrant such precision [44]. For completeness, the fits in Fig. 6(d) employing $a_c = 4.5$, 5.1 and 6.0 fm all systematically underestimate the data between $E_x = 9.61$ to 9.65 MeV. This is because these fits employ the conditions of case (4) (see Table IV) which closely mimics the fitting procedure in Ref. [21] which ignores target-related energy loss effects. By including a Landau energy loss in the experimental response, corresponding to case (5), this discrepancy is drastically reduced.

2. Isolated analysis of $^{14}\text{C}(p,t)^{12}\text{C}$ ($\theta_{\text{lab}} = 21^\circ$) data

The same systematic fitting procedure detailed in Section II C 1 was repeated for the $^{14}\text{C}(p,t)^{12}\text{C}$ ($\theta_{\text{lab}} = 21^\circ$) data which exhibits the highest resolution from the considered data of $32(1)$ keV FWHM. Furthermore, the $^{14}\text{C}(p,t)^{12}\text{C}$ ($\theta_{\text{lab}} = 21^\circ$) data exhibits the most selective population for the 3_1^- resonance relative to the surrounding 2_2^+ and monopole contributions. The same systematic trends were observed; Fig. 7 presents the corresponding fit under the same analysis conditions as Ref. [21]: case (4). Case (4) for $^{14}\text{C}(p,t)^{12}\text{C}$ ($\theta_{\text{lab}} = 21^\circ$) similarly yields $\Gamma(E_r) = 48(2)$ keV with $\Gamma_{\text{obs}}(E_r) = 38(2)$ keV. The results of this isolated analysis for the $^{14}\text{C}(p,t)^{12}\text{C}$ ($\theta_{\text{lab}} = 21^\circ$) data mirror those from the isolated analysis of the $^{12}\text{C}(p,p')^{12}\text{C}$ data. This indicates that the approximations employed in Ref. [7] are all appropriate and that the corresponding observed width of $\Gamma_{\text{obs}}(E_r) = 39(4)$

keV (converted in this work) should be included in future evaluations.

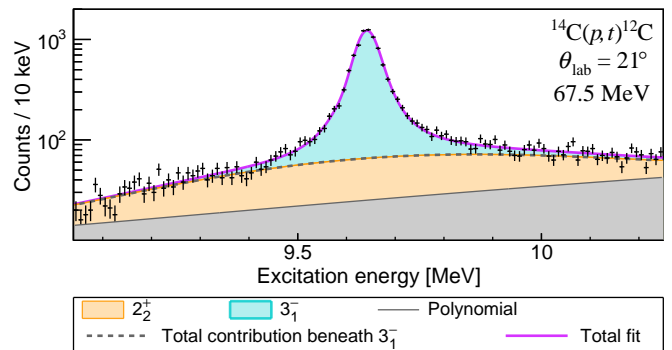


FIG. 7. (Color online) Decomposition of the fit for case (4) in Table IV. The 3_1^- resonance is superimposed on the total contribution of the 2_2^+ resonance (parameterized with a Gaussian lineshape) and a polynomial background. The reaction, measurement angle and beam energy are indicated.

D. Assessing the 3_1^- total width from Ref. [20]

The fit of the 3_1^- resonance in Ref. [20] does not employ any **R**-matrix-derived lineshapes. Instead, the fit analysis in Ref. [20] was performed with a standard/symmetric Lorentzian (that does not capture the intrinsic asymmetry of the 3_1^- resonance) which was convoluted with a Gaussian experimental resolution. The analysis in Section II C and Table IV shows that such a Lorentzian lineshape may provide a reasonable estimation of the total width, albeit possibly with a poorer quality fit. However, Ref. [20] does not implement the 2_2^+ background, which has been observed to only improve the fit, but affect the extracted 3_1^- total width. The simplified background and symmetric 3_1^- lineshape implemented by Ref. [20] thus introduces an unaccounted-for systematic error which is dependent on the relative population of the 2_2^+ and 3_1^- resonances. In this work, this systematic error is conservatively estimated by simulating the $^{10}\text{B}(^3\text{He}, p\alpha\alpha\alpha)$ and $^{11}\text{B}(^3\text{He}, d\alpha\alpha\alpha)$ spectra which correspond to Figs. 1(a) and 2(a) in Ref. [20], respectively (see Fig. 8). The simulated data was generated using two isolated (single-channel) levels: the 3_1^- resonance with $\Gamma_{\text{obs}}(E_r) = 38$ keV at $E_r = 9.641$ MeV and the 2_2^+ resonance with $\Gamma_{\text{obs}}(E_r) = 850$ keV at $E_r = 9.870$ MeV (corresponding to the current ENSDF evaluation [17]). To roughly mimic the relevant range of the $^{10}\text{B}(^3\text{He}, p\alpha\alpha\alpha)$ spectrum, the 2_2^+ and 3_1^- resonances were populated with 2.8×10^4 and 2.0×10^4 counts, respectively. Similarly for the $^{10}\text{B}(^3\text{He}, p\alpha\alpha\alpha)$ spectrum, the 2_2^+ and 3_1^- resonances are populated with 2.8×10^4 and 3.0×10^4 counts, respectively. The simulated $^{10}\text{B}(^3\text{He}, p\alpha\alpha\alpha)$ and $^{10}\text{B}(^3\text{He}, p\alpha\alpha\alpha)$ spectra were convoluted with 55 and 60 keV Gaussian resolutions, respectively (corresponding to the best resolutions for each measurement reported in

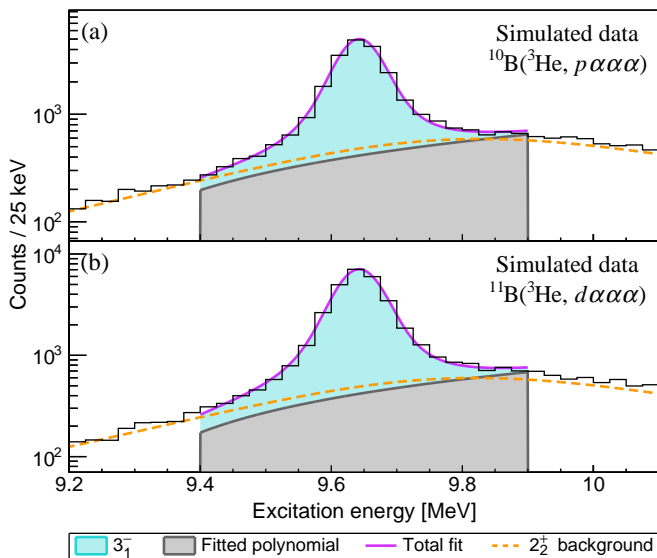


FIG. 8. (Color online) Panels (a) and (b) present simulated spectra which mimic the relevant data in Figs. 1(a) and 2(a) in Ref. [20], respectively. The purpose of this analysis is to estimate the unaccounted-for systematic error in Ref. [20]. See text for details.

Ref. [20]). The fits in Figs. 8 were performed with symmetric Lorentzian functions for the 3_1^- resonance (convoluted with the aforementioned experimental resolutions) and second-order polynomials. The total observed width of the 3_1^- resonance were extracted as 45 and 43 keV for the simulated $^{10}\text{B}(^3\text{He}, p)\alpha\alpha\alpha$ and $^{11}\text{B}(^3\text{He}, d)\alpha\alpha\alpha$ spectra, respectively. These widths are systematically higher than the simulated observed total width of 38 keV; a similar difference is observed between the optimised observed width of $\Gamma_{\text{obs}}(E_r) = 38(2)$ reported this work and the original width of $\Gamma = 43(4)$ reported in Ref. [20]. The systematic error within the 3_1^- total width extraction of Ref. [20] is therefore conservatively estimated to be $45 - 38 = 7$ keV. Adding this systematic error in quadrature yields a modified value of $\Gamma = 43(8)$ keV, which is recommended for future evaluations which consider Ref. [20].

E. Assessing the 3_1^- total width from Ref. [19]

In Ref. [19], the width of the 3_1^- resonance was obtained by fitting the spectra corresponding to the $^{10}\text{B}(^3\text{He}, p)^{12}\text{C}$ reaction. For the width of the 3_1^- resonance, the corresponding peak was directly fitted with a Lorentzian lineshape (with no Gaussian/experimental convolution). The resultant FWHM of the Lorentzian peak was assumed to correspond to the intrinsic FWHM of the 3_1^- resonance added in quadrature with the experimental resolution. This basic approximation yields a systematic error: this is tested by convoluting a $\Gamma_{\text{obs}}(E_r) = 38$ keV 3_1^- resonance with a Gaussian resolution of ≈ 100

keV FWHM observed in Fig. 2 of Ref. [19]. The numerical convolution yields an FWHM of 122 keV whilst adding the widths in quadrature yields an FWHM 107 keV. Another source of systematic error is the fitting methodology in Ref. [19] which employed a symmetric Lorentzian with no Gaussian convolution component for the experimental resolution. Finally, the underlying 2_2^+ resonance is not accounted for in Ref. [19]; a consequence of Ref. [19] being performed roughly half a century before the existence of the underlying 2_2^+ resonance was confirmed [3, 10–13]. To estimate the overall unaccounted-for systematic error from these intertwined approximations, the $^{10}\text{B}(^3\text{He}, p)^{12}\text{C}$ spectrum in Fig. 2 of Ref. [19] has been simulated in Fig. 9 of this work. As in Section IID, the simulated data employed two isolated (single-channel) levels: the 3_1^- resonance with $\Gamma_{\text{obs}}(E_r) = 38$ keV at $E_r = 9.641$ MeV and the 2_2^+ resonance with $\Gamma_{\text{obs}}(E_r) = 850$ keV at $E_r = 9.870$ MeV (corresponding to the current ENSDF evaluation [17]). To roughly mimic the $^{10}\text{B}(^3\text{He}, p)^{12}\text{C}$ data in Ref. [19], the 2_2^+ and 3_1^- resonances were each populated with 250 counts. The fitted Lorentzian yielded a total width of 110 keV and following the procedure in Ref. [19] of removing the instrumental width by “taking the square root of the difference of the squares” yields $\sqrt{110^2 - 100^2} \approx 47$ keV, producing a total systematic error of approximately $47 - 38 = 9$ keV. This systematic error is added in quadrature to the width reported in Ref. [19] to yield a modified value of $\Gamma = 36(11)$ keV, which is recommended for future evaluations which consider Ref. [19].

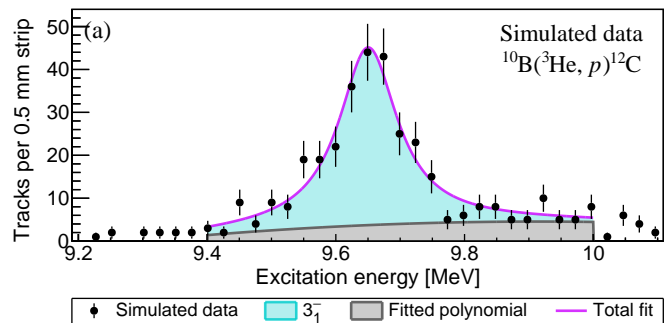


FIG. 9. (Color online) A simulated spectrum which mimics the nuclear-emulsion-plate data in Fig. 2 of Ref. [19]. The purpose of this analysis is to estimate the unaccounted-for systematic error in Ref. [19]. See text for details.

III. DISCUSSION

The primary analysis in this work (Section IIB) yields $\Gamma(E_r) = 46(2)$ keV with $\Gamma_{\text{obs}}(E_r) = 38(2)$ keV for the 3_1^- resonance in ^{12}C . The observed width from this work is significantly smaller than the current ENSDF average of $46(3)$ keV which has been employed in Ref. [15]. A meta-analysis was performed on the results currently considered in the current ENSDF evaluation [19–21] (see sec-

TABLE V. The results for the 3_1^- resonance in ^{12}C which are recommended for future ENSDF evaluations. For analyses which employed the **R**-matrix formalism, a_c denotes the channel radius. The formal, observed and FWHM widths are summarised, respectively denoted as $\Gamma(E_r)$, Γ_{obs} and Γ_{FWHM} . For the physical total widths of previous works (i.e. Γ_{obs} and Γ_{FWHM}), the total uncertainties were modified in this work.

Ref.	a_c [fm]	$\Gamma(E_r)$ [keV]	$\Gamma_{\text{obs}}(E_r)$ [keV]	Γ_{FWHM} [keV]
Browne <i>et al.</i> [19]	—	—	—	36(11)
Alcorta <i>et al.</i> [20]	—	—	—	43(8)
Kokalova <i>et al.</i> [21]	4.7 ^a	48(2)	39(4) ^b	39(4) ^b
This work	4.8	46(2)	38(2)	38(2)

^a The exact channel radius being $a_c = 1.3(4^{1/3} + 8^{1/3})$ fm [21].

^b Not reported in Ref. [21]; converted from $\Gamma(E_r)$ in this work.

tions IIC, IID and IIE). In this work, the misstated formal total width in Ref. [21] was converted to the appropriate observed total width for the ENSDF. The unaccounted-for uncertainties in Refs. [19–21] were estimated to yield modified values which we recommend for future evaluations. A quantitative assessment of Ref. [18] was deemed unfeasible within the scope of this work as the experimental methodology in Ref. [18] is significantly different from this work. However, the systematics in sections IIC, IID and IIE show that not accounting for the asymmetric background from the underlying 2_1^+ resonance gives rise to a systematic error. Therefore, until the analysis of Ref. [18] is appropriately reviewed, we recommend the associated result be omitted from future evaluations. A summary of the recommended results for the 3_1^- resonance in ^{12}C is given in Table V. To reiterate: $\Gamma_{\text{obs}}(E_r)$ and Γ_{FWHM} are equivalent for the 3_1^- resonance, see Section IIC.

The nuclear structure of the 3_1^- state also serves as an important test of theoretical models for ^{12}C . The 3_1^- state has been suggested as a candidate for the $K^\pi = 3^-$ bandhead [5, 39] and is understood to exhibit significant α -cluster structure [21] with a dominant α_0 decay mode [20, 41, 42]. Interestingly, a recent *ab initio* calculation using nuclear lattice effective field theory has predicted the 3_1^- and 2_1^+ states to exhibit equilateral triangle symmetry for the constituent alpha clusters [37]. The degree of clustering of a resonance for a particular decay partition can be gleaned from the associated Wigner ratio given by $\theta^2 = \gamma^2/\gamma_W^2$, where $\gamma_W^2 = 3\hbar^2/2\mu a_c^2$, with μ and a_c being the reduced mass and channel radius, respectively [45]. The optimal fit in Fig. 1 yields an α_0 Wigner ratio of $\approx 30\%$, which indicates a large degree

of clustering/preformation for the $^{12}\text{C} \rightarrow ^8\text{Be}(0_{\text{g.s.}}^+) + \alpha$ ($l = 3$) partition. This Wigner ratio, which is highly dependent on the channel radius, is in agreement with that reported in Ref. [21] as Kokalova *et al.* employed an α_0 channel radius of ≈ 4.7 fm, which is very similar to the optimized 4.8 fm channel radius in this work. The total observed width of $\Gamma_{\text{obs}}(E_r) = 38(2)$ is in reasonable agreement with the theoretical prediction of 30 keV by Uegaki *et al.* [46], with the total width of 68 keV predicted by Álvarez-Rodríguez *et al.* being somewhat larger [47].

IV. CONCLUSIONS

In this work, the physical total width of the 3_1^- resonance in ^{12}C was studied with a global analysis of high-resolution spectra populated with direct reactions. A simultaneous fit analysis yielded a formal total width of $\Gamma(E_r) = 46(2)$ keV and an observed total width of $\Gamma_{\text{obs}}(E_r) = 38(2)$ keV. This result is significantly discrepant with the current ENSDF average of 46(3) keV for the total width of the 3_1^- resonance [17]. To investigate this inconsistency, a meta-analysis was performed on all previous results currently considered in the current ENSDF evaluation for the 3_1^- resonance [17] (with the exception of Ref. [18]). It was concluded that all these previous results [17] contain unaccounted-for systematic errors, with a single study reporting a misstated total width [21]. An uncertainty-weighted average of the recommend observed (physical) total widths for the 3_1^- resonance yields a total width of $\Gamma_{\text{FWHM}} = 38(2)$ keV (see Table V). This physical width is recommended for future evaluations of the observed total radiative width for the 3_1^- resonance and its contribution to the high-temperature triple- α reaction rate.

ACKNOWLEDGMENTS

This work is based on the research supported in part by the National Research Foundation of South Africa (Grant Numbers: 85509, 86052, 118846, 90741). The authors acknowledge the accelerator staff of iThemba LABS for providing excellent beams. The computations were performed on resources provided by UNINETT Sigma2 - the National Infrastructure for High Performance Computing and Data Storage in Norway. K. C. W. Li would like to thank H. O. U. Fynbo, R. J. deBoer, C. R. Brune, A. C. Larsen and A. S. Voyles for useful discussions, as well as S. Basunia and J. H. Kelley for communicating details of the ENSDF evaluations.

[1] S. Hyldegaard, C. Aa. Diget, M. J. G. Borge, R. Boutami, P. Dendooven, T. Eronen, S. P. Fox, L. M. Fraile, B. R.

Fulton, H. O. U. Fynbo, J. Huikari, H. B. Jeppesen, A. S. Jokinen, B. Jonson, A. Kankainen, I. Moore, G. Nyman,

- H. Penttilä, K. Peräjärvi, K. Riisager, S. Rinta-Antila, O. Tengblad, Y. Wang, K. Wilhelmsen, and J. Äystö, Branching ratios in the β decays of ^{12}N and ^{12}B , *Phys. Rev. C* **80**, 044304 (2009).
- [2] S. Hyldegaard, M. Alcorta, B. Bastin, M. J. G. Borge, R. Boutami, S. Brandenburg, J. Büscher, P. Dendooven, C. Aa. Diget, P. Van Duppen, T. Eronen, S. P. Fox, L. M. Fraile, B. R. Fulton, H. O. U. Fynbo, J. Huikari, M. Huyse, H. B. Jeppesen, A. S. Jokinen, B. Jonson, K. Jungmann, A. Kankainen, O. S. Kirsebom, M. Madurga, I. Moore, A. Nieminen, T. Nilsson, G. Nyman, G. J. G. Onderwater, H. Penttilä, K. Peräjärvi, R. Raabe, K. Riisager, S. Rinta-Antila, A. Rogachevskiy, A. Saastamoinen, M. Sohani, O. Tengblad, E. Traykov, Y. Wang, K. Wilhelmsen, H. W. Wilschut, and J. Äystö, r -matrix analysis of the β decays of ^{12}N and ^{12}B , *Phys. Rev. C* **81**, 024303 (2010).
- [3] M. Itoh, H. Akimune, M. Fujiwara, U. Garg, N. Hashimoto, T. Kawabata, K. Kawase, S. Kishi, T. Murakami, K. Nakanishi, Y. Nakatsugawa, B. K. Nayak, S. Okumura, H. Sakaguchi, H. Takeda, S. Terashima, M. Uchida, Y. Yasuda, M. Yosoi, and J. Zenihiro, Candidate for the 2^+ excited Hoyle state at $E_x \sim 10$ MeV in ^{12}C , *Phys. Rev. C* **84**, 054308 (2011).
- [4] M. Freer and H. Fynbo, The Hoyle state in ^{12}C , *Progress in Particle and Nuclear Physics* **78**, 1 (2014).
- [5] M. Freer, H. Horiuchi, Y. Kanada-En'yo, D. Lee, and U.-G. Meißner, Microscopic clustering in light nuclei, *Rev. Mod. Phys.* **90**, 035004 (2018).
- [6] K. C. W. Li, F. D. Smit, P. Adsley, R. Neveling, P. Papka, E. Nikolskii, J. Brümmer, L. Donaldson, M. Freer, M. N. Harakeh, F. Nemulodi, L. Pellegri, V. Pseudo, M. Wiedeking, E. Z. Buthelezi, V. Chudoba, S. V. Förtsch, P. Jones, M. Kamil, J. P. Mira, G. G. O'Neill, E. Sideras-Haddad, B. Singh, S. Siem, G. F. Steyn, J. A. Swartz, I. Usman, and J. van Zyl, Investigating the predicted breathing-mode excitation of the Hoyle state, *Physics Letters B* **827**, 136928 (2022).
- [7] K. C. W. Li, P. Adsley, R. Neveling, P. Papka, F. D. Smit, E. Nikolskii, J. W. Brümmer, L. M. Donaldson, M. Freer, M. N. Harakeh, F. Nemulodi, L. Pellegri, V. Pseudo, M. Wiedeking, E. Z. Buthelezi, V. Chudoba, S. V. Förtsch, P. Jones, M. Kamil, J. P. Mira, G. G. O'Neill, E. Sideras-Haddad, B. Singh, S. Siem, G. F. Steyn, J. A. Swartz, I. T. Usman, and J. J. van Zyl, Multiprobe study of excited states in ^{12}C : Disentangling the sources of monopole strength between the energy of the Hoyle state and $E_x = 13$ MeV, *Phys. Rev. C* **105**, 024308 (2022).
- [8] C. Angulo, M. Arnould, M. Rayet, P. Descouvemont, D. Baye, C. Leclercq-Willain, A. Coc, S. Barhoumi, P. Aguer, C. Rolfs, R. Kunz, J. Hammer, A. Mayer, T. Paradellis, S. Kossionides, C. Chronidou, K. Spyrou, S. Degl'Innocenti, G. Fiorentini, B. Ricci, S. Zavatarelli, C. Providencia, H. Wolters, J. Soares, C. Grama, J. Rahighi, A. Shotter, and M. Laméhi Rachti, A compilation of charged-particle induced thermonuclear reaction rates, *Nuclear Physics A* **656**, 3 (1999).
- [9] H. O. U. Fynbo, C. Aa. Diget, U. C. Bergmann, M. J. G. Borge, J. Cederkäll, P. Dendooven, L. M. Fraile, S. Franchoo, V. N. Fedosseev, B. R. Fulton, W. Huang, J. Huikari, H. B. Jeppesen, A. S. Jokinen, P. Jones, B. Jonson, U. Köster, K. Langanke, M. Meister, T. Nilsson, G. Nyman, Y. Prezado, K. Riisager, S. Rinta-Antila, O. Tengblad, M. Turrion, Y. Wang, L. Weissman, K. Wilhelmsen, J. Äystö, and The ISOLDE Collaboration, Revised rates for the stellar triple- α process from measurement of ^{12}C nuclear resonances, *Nature* **433**, 136 (2005).
- [10] M. Itoh, H. Akimune, M. Fujiwara, U. Garg, H. Hashimoto, T. Kawabata, K. Kawase, S. Kishi, T. Murakami, K. Nakanishi, Y. Nakatsugawa, B. K. Nayak, S. Okumura, H. Sakaguchi, H. Takeda, S. Terashima, M. Uchida, Y. Yasuda, M. Yosoi, and J. Zenihiro, Study of the cluster state at $e_x = 10.3$ MeV in ^{12}C , *Proceedings of the 8th International Conference on Clustering Aspects of Nuclear Structure and Dynamics*, *Nuclear Physics A* **738**, 268 (2004).
- [11] M. Freer, H. Fujita, Z. Buthelezi, J. Carter, R. W. Fearick, S. V. Förtsch, R. Neveling, S. M. Perez, P. Papka, F. D. Smit, J. A. Swartz, and I. Usman, 2^+ excitation of the ^{12}C Hoyle state, *Phys. Rev. C* **80**, 041303 (2009).
- [12] M. Freer, M. Itoh, T. Kawabata, H. Fujita, H. Akimune, Z. Buthelezi, J. Carter, R. W. Fearick, S. V. Förtsch, M. Fujiwara, U. Garg, N. Hashimoto, K. Kawase, S. Kishi, T. Murakami, K. Nakanishi, Y. Nakatsugawa, B. K. Nayak, R. Neveling, S. Okumura, S. M. Perez, P. Papka, H. Sakaguchi, Y. Sasamoto, F. D. Smit, J. A. Swartz, H. Takeda, S. Terashima, M. Uchida, I. Usman, Y. Yasuda, M. Yosoi, and J. Zenihiro, Consistent analysis of the 2^+ excitation of the ^{12}C Hoyle state populated in proton and α -particle inelastic scattering, *Phys. Rev. C* **86**, 034320 (2012).
- [13] W. R. Zimmerman, M. W. Ahmed, B. Bromberger, S. C. Stave, A. Breskin, V. Dangendorf, T. Delbar, M. Gai, S. S. Henshaw, J. M. Mueller, C. Sun, K. Tittelmeier, H. R. Weller, and Y. K. Wu, Unambiguous identification of the second 2^+ state in ^{12}C and the structure of the Hoyle state, *Phys. Rev. Lett.* **110**, 152502 (2013).
- [14] D. Chamberlin, D. Bodansky, W. W. Jacobs, and D. L. Oberg, Upper limit on the radiative width of the 9.64-MeV state of ^{12}C , *Phys. Rev. C* **10**, 909 (1974).
- [15] M. Tsumura, T. Kawabata, Y. Takahashi, S. Adachi, H. Akimune, S. Ashikaga, T. Baba, Y. Fujikawa, H. Fujimura, H. Fujioka, T. Furuno, T. Hashimoto, T. Harada, M. Ichikawa, K. Inaba, Y. Ishii, N. Itagaki, M. Itoh, C. Iwamoto, N. Kobayashi, A. Koshikawa, S. Kubono, Y. Maeda, Y. Matsuda, S. Matsumoto, K. Miki, T. Morimoto, M. Murata, T. Nanamura, I. Ou, S. Sakaguchi, A. Sakaue, M. Sferrazza, K. Suzuki, T. Takeda, A. Tamii, K. Watanabe, Y. Watanabe, H. Yoshida, and J. Zenihiro, First experimental determination of the radiative-decay probability of the 3_1^- state in ^{12}C for estimating the triple alpha reaction rate in high temperature environments, *Physics Letters B* **817**, 136283 (2021).
- [16] H. Crannell, T. Griffy, L. Suelzle, and M. Yearian, A determination of the transition widths of some excited states in ^{12}C , *Nuclear Physics A* **90**, 152 (1967).
- [17] J. Kelley, J. Purcell, and C. Sheu, Energy levels of light nuclei $a=12$, *Nuclear Physics A* **968**, 71 (2017).
- [18] R. A. Douglas, J. W. Broer, R. Chiba, D. F. Herring, and E. A. Silverstein, Electrostatic analysis of nuclear reaction energies, *Phys. Rev.* **104**, 1059 (1956).
- [19] C. P. Browne, W. E. Dorenbusch, and J. R. Erskine, High-resolution study of the $\text{B}^{10}(\text{He}^3, p)\text{C}^{12}$ reaction, *Phys. Rev.* **125**, 992 (1962).
- [20] M. Alcorta, M. J. G. Borge, M. Cubero, C. A. Diget, R. Domínguez-Reyes, L. M. Fraile, B. R. Fulton, H. O. U. Fynbo, D. Galaviz, S. Hyldegaard, H. Jeppesen, B. Jon-

- son, O. S. Kirsebom, M. Madurga, A. Maira, A. Muñoz Martín, T. Nilsson, G. Nyman, D. Obradors, A. Perea, K. Riisager, O. Tengblad, and M. Turrion, Properties of ^{12}C resonances determined from the $^{10}\text{B}(^3\text{He}, p\alpha\alpha)$ and $^{11}\text{B}(^3\text{He}, d\alpha\alpha\alpha)$ reactions studied in complete kinematics, *Phys. Rev. C* **86**, 064306 (2012).
- [21] Tz. Kokalova, M. Freer, Z. Buthelezi, J. Carter, R. W. Fearick, S. V. Förtsch, H. Fujita, R. Neveling, P. Papka, F. D. Smit, J. A. Swartz, and I. Usman, Precision measurement of the 9.641 MeV, 3^- state in ^{12}C , *Phys. Rev. C* **87**, 057307 (2013).
- [22] J. H. Kelley, *Private communications* (2023).
- [23] J. K. Tuli, *Evaluated Nuclear Structure Data File, A Manual for Preparation of Datasets*, <https://nds.iaea.org/public/documents/ensdf/ensdf-manual.pdf>.
- [24] M. Birch, *Visual Averaging Library (V.AveLib) User Manual*, https://github.com/IAEA-NSDDNetwork/V.AveLib/blob/main/AveLib_userManual.pdf.
- [25] G. Cardella, F. Favela, N. S. Martorana, L. Acosta, A. Camaiani, E. De Filippo, N. Gelli, E. Geraci, B. Gnoffo, C. Guazzoni, G. Immè, D. J. Marín-Lámbarri, G. Lanzalone, I. Lombardo, L. Lo Monaco, C. Maiolino, A. Nannini, A. Pagano, E. V. Pagano, M. Papa, S. Pirrone, G. Politi, E. Pollacco, L. Quattrocchi, F. Risitano, F. Rizzo, P. Russotto, V. L. Sicari, D. Santonocito, A. Trifirò, and M. Trimarchi, Investigating γ -ray decay of excited ^{12}C levels with a multifold coincidence analysis, *Phys. Rev. C* **104**, 064315 (2021).
- [26] G. Breit and M. E. Ebel, Nucleon transfer and virtual Coulomb excitation, *Phys. Rev.* **104**, 1030 (1956).
- [27] A. M. Lane and R. G. Thomas, R-matrix theory of nuclear reactions, *Rev. Mod. Phys.* **30**, 257 (1958).
- [28] R. J. deBoer, J. Görres, M. Wiescher, R. E. Azuma, A. Best, C. R. Brune, C. E. Fields, S. Jones, M. Pignatari, D. Sayre, K. Smith, F. X. Timmes, and E. Uberseder, The $^{12}\text{C}(\alpha, \gamma)^{16}\text{O}$ reaction and its implications for stellar helium burning, *Rev. Mod. Phys.* **89**, 035007 (2017).
- [29] C. R. Brune, Spectroscopic factors, overlaps, and isospin symmetry from an R -matrix point of view, *Phys. Rev. C* **102**, 034328 (2020).
- [30] C. R. Brune, Alternative parametrization of r -matrix theory, *Phys. Rev. C* **66**, 044611 (2002).
- [31] P. Ducru and V. Sobes, Definite complete invariant parametrization of r -matrix theory, *Phys. Rev. C* **105**, 024601 (2022).
- [32] C. Kurokawa and K. Katō, New broad 0^+ state in ^{12}C , *Phys. Rev. C* **71**, 021301 (2005).
- [33] C. Kurokawa and K. Katō, Spectroscopy of ^{12}C within the boundary condition for three-body resonant states, *Nuclear Physics A* **792**, 87 (2007).
- [34] S.-I. Ohtsubo, Y. Fukushima, M. Kamimura, and E. Hiyama, Complex-scaling calculation of three-body resonances using complex-range Gaussian basis functions: Application to 3α resonances in ^{12}C , *Progress of Theoretical and Experimental Physics* **2013**, 10.1093/ptep/ptt048 (2013), 073D02, <http://oup.prod.sis.lan/ptep/article-pdf/2013/7/073D02/19300448/ptt048.pdf>.
- [35] B. Zhou, A. Tohsaki, H. Horiuchi, and Z. Ren, Breathing-like excited state of the Hoyle state in ^{12}C , *Phys. Rev. C* **94**, 044319 (2016).
- [36] H. Takemoto, T. Myo, H. Horiuchi, H. Toki, M. Isaka, M. Lyu, Q. Zhao, and N. Wan, Appearance of the Hoyle state and its breathing mode in ^{12}C despite strong short-range repulsion of the nucleon-nucleon potential, *Phys. Rev. C* **107**, 044304 (2023).
- [37] S. Shen, S. Elhatisari, T. A. Lähde, D. Lee, B.-N. Lu, and U.-G. Meißner, Emergent geometry and duality in the carbon nucleus, *Nature Communications* **14**, 2777 (2023).
- [38] E. Uegaki, S. Okabe, Y. Abe, and H. Tanaka, Structure of the Excited States in ^{12}C , *Progress of Theoretical Physics* **57**, 1262 (1977), <https://academic.oup.com/ptp/article-pdf/57/4/1262/5447216/57-4-1262.pdf>.
- [39] Y. Kanada-En'yo, Variation after angular momentum projection for the study of excited states based on antisymmetrized molecular dynamics, *Phys. Rev. Lett.* **81**, 5291 (1998).
- [40] T. Neff and H. Feldmeier, Cluster structures within fermionic molecular dynamics, *Nuclear Physics A* **738**, 357 (2004), proceedings of the 8th International Conference on Clustering Aspects of Nuclear Structure and Dynamics.
- [41] M. Freer, I. Boztosun, C. A. Bremner, S. P. G. Chappell, R. L. Cowin, G. K. Dillon, B. R. Fulton, B. J. Greenhalgh, T. Munoz-Britton, M. P. Nicoli, W. D. M. Rae, S. M. Singer, N. Sparks, D. L. Watson, and D. C. Weissler, Reexamination of the excited states of ^{12}C , *Phys. Rev. C* **76**, 034320 (2007).
- [42] J. Manfredi, R. J. Charity, K. Mercurio, R. Shane, L. G. Sobotka, A. H. Wuosmaa, A. Banu, L. Trache, and R. E. Tribble, α decay of the excited states in ^{12}C at 7.65 and 9.64 MeV, *Phys. Rev. C* **85**, 037603 (2012).
- [43] M. Galassi *et al.*, *GNU Scientific Library Reference Manual (3rd Ed.)*, ISBN 0954612078.
- [44] N. Michel, Precise coulomb wave functions for a wide range of complex l , η and z , *Computer Physics Communications* **176**, 232 (2007).
- [45] T. Teichmann and E. P. Wigner, Sum rules in the dispersion theory of nuclear reactions, *Phys. Rev.* **87**, 123 (1952).
- [46] E. Uegaki, Y. Abe, S. Okabe, and H. Tanaka, Structure of the Excited States in ^{12}C . II, *Progress of Theoretical Physics* **62**, 1621 (1979), <http://oup.prod.sis.lan/ptp/article-pdf/62/6/1621/5398938/62-6-1621.pdf>.
- [47] R. Álvarez-Rodríguez, E. Garrido, A. S. Jensen, D. V. Fedorov, and H. O. U. Fynbo, Structure of low-lying ^{12}C resonances, *The European Physical Journal A* **31**, 303 (2007).